J Mater Sci (2010) 45:3228–3241
DOI 10.1007/s10853-010-4330-x

Statistical quantification of the microstructural homogeneity of size and orientation distributions

Z. P. Luo

Received: 2 October 2009 / Accepted: 16 February 2010 / Published online: 12 March 2010

Abstract Methodologies to quantify the microstructural homogeneity, or uniformity, have been developed based on the proposed statistical homogeneity theory. Two kinds of homogeneities are considered, for the size and orientation distributions, respectively. In the case of size distribution, the homogeneity is quantified using two parameters, $H_{0.1}$ and $H_{0.2}$, which are defined as the probabilities falling into the ranges of $\mu \pm 0.1\mu$ and $\mu \pm 0.2\mu$, respectively, where μ is the mean size. Whereas in the case of orientation distribution, three parameters are used to quantify the homogeneity: H_R, the mean resultant length that is a simple measure of the angular data concentration, and $H_{0.1}$ and $H_{0.2}$, which are the probabilities in particular angular ranges of the circular or spherical data. These homogeneity quantities are formularized using the common statistical models, and typical examples are demonstrated.

List of symbols

a, b, c	Grain axes
COV or σ/μ	Coefficient of variation
COV(d_{mean})	Coefficient of variation of the mean near-neighbor distance
$(\overline{C}, \overline{S})$	Coordinates of mean resultant vector
D, $D_{0.1}$ and $D_{0.2}$	Dispersion quantities
f	Probability density function
G_v	Grain homogeneity parameter
H, $H_{0.1}$ and $H_{0.2}$	Homogeneity quantities
H_R	Directional homogeneity quantity
HPq	Dimensionless homogeneity parameter
K	Curvature
L	Length
N	Total number, or measurement number
p	Fitting parameter
$\overline{R}$	Mean resultant length
r	Correlation coefficient
s	Sample standard deviation
U_{size}	Size uniformity
U_{sp}	Spatial uniformity
$\overline{V}$	Mean volume
$\overline{x}$	Sample mean
(x, y)	Mass center
(x_G, y_G)	Mass gravity center
(x_S, y_S)	Microstructural center
α and β	Fitting parameters
ϕ	Longitude
κ	Fitting parameter
μ	Population mean
θ	Angle, or colatitude
ρ	Population mean resultant length
σ	Population standard deviation
σ_{ga}	Standard deviation of the grain areas

Z. P. Luo (✉)
Microscopy and Imaging Center, Texas A&M University, College Station, TX 77843-2257, USA
e-mail: luo@mic.tamu.edu

Introduction

Currently, the material microstructures are widely studied by different microscopy techniques, such as light microscopy, transmission (TEM), and scanning electron microscopy. With the aid of standards, it is possible to accurately measure the dimension of the features, with resolutions at several ångström levels in a conventional TEM. In order to analyze the size distribution, the measurements should be made on sufficient sampling. The available image processing techniques, based on the threshold method, have made it possible to provide the feature dimensions

(diameter, perimeter, and area), mass center coordinates (x, y), angles, and the volume or area fractions, based on a large number of measurements.

Quantification of the material microstructure can provide a better understanding of the microstructure–property relationship [1]. One of the quantification issues is the evaluation of the microstructural homogeneity, or uniformity. For example, if samples contain grains or particles with different size, it is necessary to establish certain standards to quantitatively compare their homogeneity degrees. In the past, this homogeneity was quantified in the following ways.

(1) Takayama et al. [2] proposed size uniformity U_{size} and spatial uniformity U_{sp} to quantify the uniformity of grain microstructure. The U_{size} is defined as:

$$U_{\text{size}} = 1/\sigma_{\text{ga}}, \tag{1}$$

where σ_{ga} is the standard deviation of the grain areas of the intersection. To obtain U_{sp}, a square area with length L is selected, and then the area of each grain a_i and its mass center (x_i, y_i) are measured to obtain the mass gravity center $(x_{\text{G}}, y_{\text{G}})$ and the microstructural center $(x_{\text{S}}, y_{\text{S}})$ as follows:

$$x_{\text{G}} = \sum x_i a_i / \sum a_i,\ y_{\text{G}} = \sum y_i a_i / \sum a_i, \tag{2a}$$

$$x_{\text{S}} = \sum x_i a_i^2 / \sum a_i^2,\ y_{\text{S}} = \sum y_i a_i^2 / \sum a_i^2. \tag{2b}$$

Afterward, U_{sp} is defined as

$$U_{\text{sp}} = 1 - \sqrt{2[(x_{\text{G}} - x_{\text{S}})^2 + (y_{\text{G}} - y_{\text{S}})^2]}/L. \tag{3}$$

It was found that these two parameters U_{size} and U_{sp} were useful to quantify the grain size uniformity of pure iron samples.

(2) A dimensionless homogeneity parameter HPq, the coefficient of variation (COV), was proposed by Heijman and coworkers [3, 4] to quantify the homogeneity of particles as follows:

$$\text{HP}_q = \sigma_q/\mu_q. \tag{4}$$

Here, $\mu_q = \frac{1}{N}\sum_{i=1}^{N} q_i$ and $\sigma_q = \sqrt{\sum_{i=1}^{N}(q_i - \mu_q)^2/(N-1)}$ are the mean and standard deviation of the property q over the total number N. The property q can be area, perimeter, or number of faces of a polygon.

(3) A parameter G_{v}, proposed by Sidor et al. [5, 6], was used to quantify the grain homogeneity. It is defined as:

$$G_{\text{V}} = \frac{\overline{V}}{\frac{4}{3}\pi\,\overline{a}\,\overline{b}\,\overline{c}} = N^2 \frac{\sum_{i=1}^{N} a_i b_i c_i}{\sum_{i=1}^{N} a_i \sum_{i=1}^{N} b_i \sum_{i=1}^{N} c_i}, \tag{5}$$

where $\overline{V}$ is the mean volume of grains, N the total number of grains, and a_i, b_i, c_i the Cartesian axes of the ith grain.

In addition to the feature size, their orientation distribution is another important fact to be considered in the microstructural quantification. Typical examples are: the alignment of reinforcements in fabric composite materials [7–9], grain alignment or misorientation angles [10], crystallographic orientation between different phases [11], orientation in wood structures [12], etc. Such orientation distribution may play an important role in influencing the material performance. An early work by Rigdahl et al. [13] studied the elastic behavior of low-density paper. They found that the paper elastic properties are related to the sheet density, fiber modulus, mean fiber length, and fiber orientation; and the orthortropic elastic parameters could be estimated by the observed orientation data using von Mises mathematical model with a good agreement. Later, Schulgasser processed their experimental data using wrapped Cauchy model to reveal the relationship between the mechanical behavior and fiber orientation distribution [14]. In composite materials, the orientation distribution of reinforcements, such fibers, affects the material mechanical properties significantly. Fu and Lauke [8] found that both of the fiber length and the fiber orientation distribution had impact on the composite strength, which increased with an increase of fiber orientation coefficient, or a decrease of the fiber mean orientation angle. As compared to the size distribution, much less efforts were made so far to quantify the homogeneity degree of the orientation distribution dealing with the angular data.

The previous quantifications were made using specified parameters to quantify a particular material case. The aim of this work is to develop a statistical homogeneity theory to provide more general methodologies to quantify the homogeneity degrees from the statistical approach, without any restrictions of the sample type, such as grains or particles. It focuses on two major important parts of the microstructures, including the size and orientation distributions, respectively. The methodologies are given below along with typical examples, while the detailed particular statistical models and formularizations are placed in Appendices 1 and 2 for reference.

Methodology for the size distribution

In material microstructure, it is often needed to measure the size of features using different approaches [15–22]. Based on such size measurements, one may establish a histogram to elucidate the size distribution using the probability density function (PDF), $f(x)$. If the number of measurements N is sufficiently large, the sample mean $\overline{x}$ and sample standard deviation s may be used to estimate the population mean μ and the population standard deviation σ, respectively, i.e., $\hat{\mu} = \overline{x}$ and $\hat{\sigma} = s$, where $\hat{\mu}$ and $\hat{\sigma}$ are the

estimators of μ and σ, respectively. It is apparent that the size distribution character is related to σ, as a lower σ makes a higher degree of homogeneity. However, the quantity σ is not a good measure of the homogeneity degree, as it has the same unit of the size, and thus the homogeneity degrees of measurements in different units are not comparable using σ. Only with the same μ, the homogeneity degree can be compared through σ.

Consider a data distribution $f(x)$ with mean μ in the entire range, we may define the homogeneity degree as the probability within a certain data range around μ, and thus two quantities $H_{0.1}$ and $H_{0.2}$, in the range of $\mu \pm 0.1\mu$ and $\mu \pm 0.2\mu$, respectively, are obtained as follows:

$$H_{0.1} = \int_{0.9\mu}^{1.1\mu} f(x) \cdot \mathrm{d}x, \; H_{0.2} = \int_{0.8\mu}^{1.2\mu} f(x) \cdot \mathrm{d}x. \tag{6}$$

By this theoretical definition, the homogeneity quantities, $H_{0.1}$ and $H_{0.2}$, are the areas under PDF in the $\mu \pm 0.1\mu$ and $\mu \pm 0.2\mu$ range, respectively. A distribution with higher degree of data concentration, i.e., less σ, would possess higher PDF around μ, and thus it possesses higher H values according to this definition. Note that $H_{0.1}$ and $H_{0.2}$ are dimensionless quantities, and thus it is possible to compare the homogeneity degrees of measurements in different units through $H_{0.1}$ and $H_{0.2}$. The previous definition of the dispersion quantity D [23] is indeed a special case of the homogeneity—the free-path spacing homogeneity.

In the past, different mathematical models have been applied to simulate the size distribution. Probably, the mostly used models are normal, lognormal, gamma, and Weibull distributions [17]. According to these statistical models [24], the homogeneity degrees $H_{0.1}$ and $H_{0.2}$ are deduced relating to μ and σ, see Appendix 1, for details. It is found that for the normal, lognormal, gamma (including its special cases of the Erlang and chi-square), and Weibull (including its special case of Rayleigh) distributions, the $H_{0.1}$ and $H_{0.2}$ are monotonic increasing functions, with the only variable of the ratio μ/σ, as plotted in Fig. 1. A higher μ, or a lower σ, would result in higher H values. This is consistent to the fact that from the measurement point of view, larger objects look more homogeneous as compared to the smaller objects with the same σ. For example, particles with size 10 ± 5 nm look inhomogeneous, while particles 10 μm ± 5 nm (with the same standard deviation) look very homogeneous. In the extreme case, when $\mu \to \infty$ or $\sigma \to 0, H \to 100\%$. To calculate $H_{0.1}$ and $H_{0.2}$ values using the formulas listed in Appendix 1, one may use the sample mean $\bar{x} = \sum_i x_i/N$ and data sample standard deviation $s = \sqrt{\sum_i (x_i - \bar{x})^2/(N-1)}$ to estimate the population mean μ and population standard deviation σ,

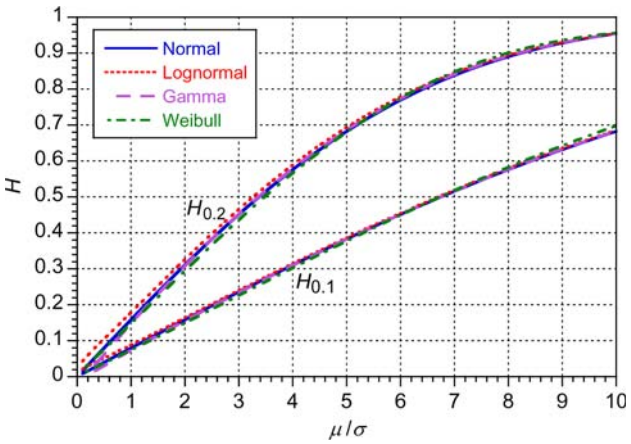

Fig. 1 Homogeneity quantities $H_{0.1}$ and $H_{0.2}$ as a function of μ/σ

respectively, if the number of measurements N is sufficiently large, typically $N > 100$.

As mentioned in the introduction, Heijman et al. [3, 4] used the ratio $\mathrm{HP}_q = \sigma_q/\mu_q$ as a homogeneity quantification parameter, which has indeed an opposite meaning of H, i.e., the lower HP_q value means the higher homogeneity, as HP_q is in the reciprocal form of the ratio μ/σ used for the quantification in this article. This work proves that such a comparison by the ratio is correct for most of the distribution models. However, as given in Appendix 1, for some distributions, for example, the beta distribution when $\alpha \neq \beta$, the ratio μ/σ is not always the only variable of H. In this case, the H functions are no longer monotonic and thus they have different values for a given ratio μ/σ. Therefore, the comparison of the homogeneity degree through the ratio, either HPq or μ/σ, is invalid. However, the homogeneity degrees defined through the integrations, as expressed in Eq. 6, are not restricted to the monotonicity nature of the functions. As a general way, one may calculate the H values numerically by the integrating the measured $f(x)$ as defined in Eq. 6, even without knowing the statistical model.

In addition to the homogeneity degree of size distribution studied here, previous nearest-neighbour distance measurements were performed to evaluate the microstructural homogeneity of the spatial distribution of secondary phase particles [25]. Yang et al. [26] proposed that the coefficient of variation of the mean near-neighbour distance, $\mathrm{COV}(d_{\mathrm{mean}})$, is a powerful parameter to identify the microstructural homogeneity of particulate/metal matrix composites. For a homogenous (or random) distribution, $\mathrm{COV}(d_{\mathrm{mean}}) = 0.36$, which increases with increasing the inhomogeneity of clustering. Another approach on the homogeneity of reinforcement distribution was performed by Ganguly and Poole [27]. In fact, the evaluation of clustering may be related to the particle spatial dispersion,

which was studied recently [23, 28, 29]. As the dispersion quantification is a special case of the free-path spacing homogeneity, the results presented in Appendix 1 also serve as a supplemental work to the earlier dispersion quantification [23].

Methodology for the orientation distribution

Distribution of 2-D circular data

Circular data are angles in the 2-D space, including axial data (vary from 0 to π) and directional data (vary from 0 to 2π). Schematic examples of the axial data are shown in Fig. 2a, b, where the linear features align well along a direction (the mean direction) in Fig. 2a, but align in a less degree in Fig. 2b. As θ and $\theta + \pi$ are equivalent, the measured θ angle range is π. The angle distribution is plotted on the unit circle in Fig. 2c, which only covers a half circle. Each point on the circle represents an orientation angle.

The directional data examples are given in Fig. 2d, e, where the feature directions are considered in Fig. 2d, or the tangent direction distribution along a curve in Fig. 2e. Here, the measured angle θ range is 2π. The angle distribution is plotted on the circle in Fig. 2f, which covers the full circle.

The quantification of angular data, either axial or directional, requires circular statistics [30–33]. An arbitrary angle θ, can be regarded as a unit vector $\mathbf{X}$; or as a point on the unit circle, with Cartesian coordinates of $\cos\theta$ and $\sin\theta$. By measuring the angle θ_i ($i = 1, 2, \ldots, N$) of a number of features, the mean direction $\overline{\theta}$ is the direction of the resultant vector, $\mathbf{R} = \mathbf{X}_1 + \mathbf{X}_2 + \cdots + \mathbf{X}_N$, with a resultant length R. Dividing this vector $\mathbf{R}$ by the number N yields the mean resultant vector $\overline{\mathbf{R}}$ with length $\overline{R}$, whose coordinates are

$$\overline{C} = \frac{1}{N}\sum_{j=1}^{N}\cos\theta_j,\ \overline{S} = \frac{1}{N}\sum_{j=1}^{N}\sin\theta_j. \tag{7}$$

Thus,

$$\overline{R} = \sqrt{\overline{C}^2 + \overline{S}^2},\ \overline{\theta} = \begin{cases} \tan^{-1}(\overline{S}/\overline{C}) & \text{if } \overline{C} \geq 0, \\ \tan^{-1}(\overline{S}/\overline{C}) + \pi & \text{if } \overline{C} < 0. \end{cases} \tag{8}$$

The mean resultant length $\overline{R}$ is a measure of the circular data concentration, and $0 \leq \overline{R} \leq 1$. When $\overline{R} = 0, \overline{\theta}$ is not defined, which is the case of uniform (or random) distribution; and if all θ_i angles are the same, $\overline{R} = 1$. This mean resultant length value may be used to quantify the homogeneity degree, that is,

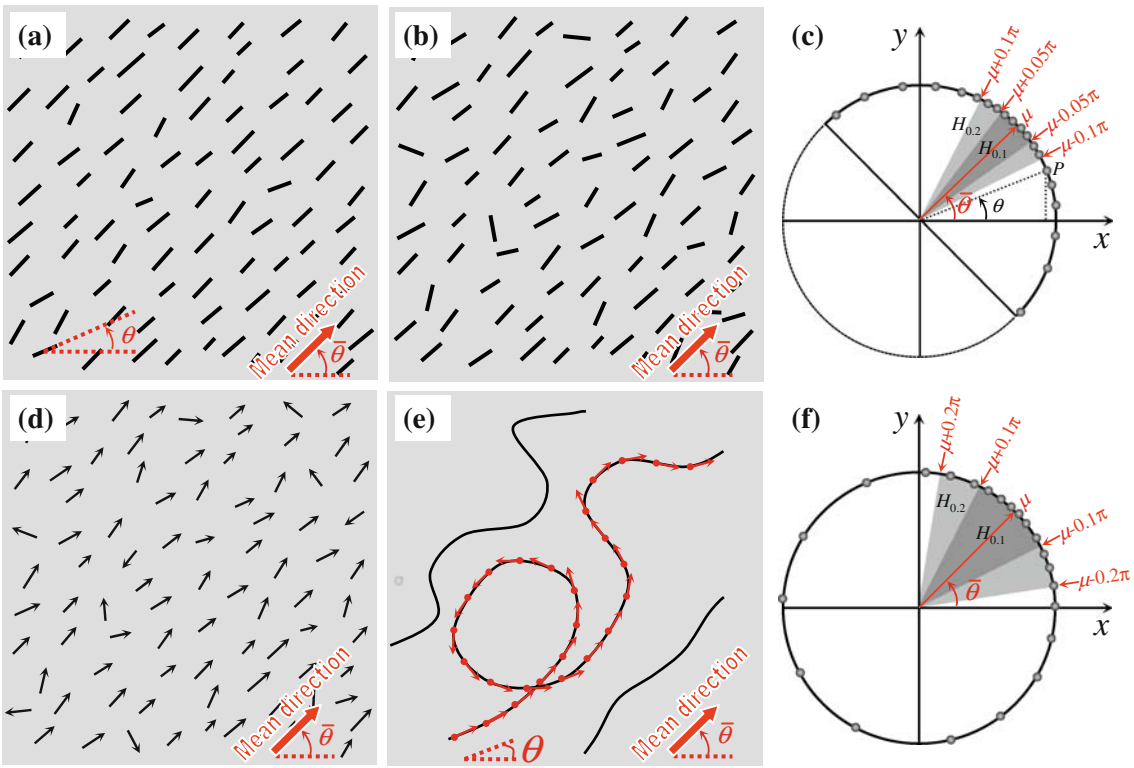

Fig. 2 Schematic microstructures showing orientation distributions. **a** The linear features align well along the mean direction; **b** linear features do not aligned well; **c** orientation distribution of axial data on the half circle; **d** alignment of directional lines; **e** directions of tangent lines; **f** orientation distribution of directional data on the full circle

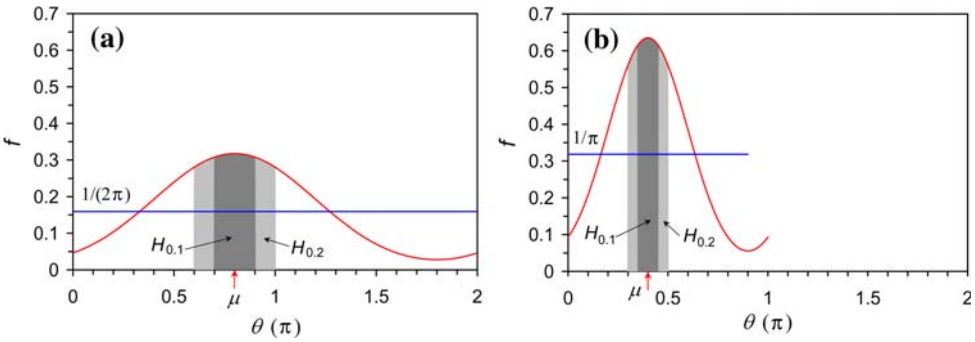

Fig. 3 Definition of $H_{0.1}$ and $H_{0.2}$ of the angular distribution, when $0 \le \theta < 2\pi$ for directional data (**a**) and $0 \le \theta < \pi$ for axial data (**b**). The PDF's of uniform (random) distributions are the horizontal straight lines

$$H_R = \overline{R}. \tag{9}$$

Accordingly, $0 \le H_R \le 1$. Here, we use the sample mean resultant length $\overline{R}$ to estimate the population mean resultant length ρ, assuming the measurement number N is sufficiently large.

An alternative way to quantify the homogeneity is to define the homogeneity from the PDF $f(\theta)$ of the circular data, which is similar to the size distribution. For the directional data, $0 \le \theta < 2\pi$, $f(\theta)$ has the following properties: $f(\theta) \ge 0; f(\theta) = f(\theta + 2\pi)$; and $\int_0^{2\pi} f(\theta)\,\mathrm{d}\theta = 1$. As shown in Fig. 3a, we define the homogeneity quantities, $H_{0.1}$ and $H_{0.2}$, as the probabilities in the range of $\mu \pm 0.1\pi$ and $\mu \pm 0.2\pi$, respectively,

$$H_{0.1} = \int_{\mu-0.1\pi}^{\mu+0.1\pi} f(\theta)\,\mathrm{d}\theta,\ H_{0.2} = \int_{\mu-0.2\pi}^{\mu+0.2\pi} f(\theta)\,\mathrm{d}\theta. \tag{10}$$

Here, μ is the mean direction of the distribution. For the uniform (or random) distribution, $f(\theta) = 1/(2\pi)$ is a constant, as shown by the horizontal straight line in Fig. 3a, thus $H_{0.1}$=0.1 and $H_{0.2}$=0.2 under this definition, which mean that there are 0.1 and 0.2 possibilities of the data distributed in within $\mu \pm 0.1\pi$ and $\mu \pm 0.2\pi$, respectively. Hence, $0.1 \le H_{0.1} \le 1$, and $0.2 \le H_{0.2} \le 1$.

Consider the axial data, with $0 \le \theta < \pi$. $f(\theta)$ obeys: $f(\theta) \ge 0; f(\theta) = f(\theta + \pi)$; and $\int_0^{\pi} f(\theta)\,\mathrm{d}\theta = 1$. Since the angle range $[0, \pi)$ is reduced half as compared to directional data range $[0, 2\pi)$, $H_{0.1}$ and $H_{0.2}$ are defined the probabilities in the range of $\mu \pm 0.05\pi$ and $\mu \pm 0.1\pi$, respectively (Fig. 3b),

$$H_{0.1} = \int_{\mu-0.05\pi}^{\mu+0.05\pi} f(\theta)\,\mathrm{d}\theta,\ H_{0.2} = \int_{\mu-0.1\pi}^{\mu+0.1\pi} f(\theta)\,\mathrm{d}\theta. \tag{11}$$

Note that in the axial data case, since θ and $\theta + \pi$ are equivalent, its probability is doubled as compared to the directional data. Therefore, $H_{0.1}$ and $H_{0.2}$ values, or the shadowed areas in Fig. 3a and b, respectively, remain the same for directional or axial data. In fact, doubling the angles of the axial data converts them to the directional data.

The quantities H_R, $H_{0.1}$, and $H_{0.2}$ are three different parameters that measure the homogeneity degree in different ways. Considering the common wrapped normal, wrapped Cauchy, von Mises, cardioid, and triangle distributions, H_R, $H_{0.1}$, and $H_{0.2}$ are formularized in Appendix 2. As shown in Figs. 9, 10, 11, 12, all three parameters are monotonic functions of specific parameters, so that each of them can quantify the homogeneity degree consistently.

Distribution of 3-D spherical data

Similar to the 2-D orientation data distribute on the unit circle, the orientation data in the 3-D space distribute on the unit sphere [34–36], as shown in Fig. 4. The coordinates of an arbitrary orientation point, P, are denoted as colatitude θ ($0 \le \theta \le \pi$), and longitude ϕ ($0 \le \phi < 2\pi$). Rotate the system coordinate so that the mean orientation point μ reaches the z axis with its $\theta = 0$. Therefore, similar to the 2-D circular data, the homogeneity is quantified by the distribution around the mean orientation. Note that the element area of the sphere surface is $\mathrm{d}S = \sin\theta\,\mathrm{d}\theta\,\mathrm{d}\varphi$. As $0 \le \phi < 2\pi$, we define $H_{0.1}$ and $H_{0.2}$ are the probabilities only with θ as the variable from 0 to 0.1π and from 0 to 0.2π, respectively,

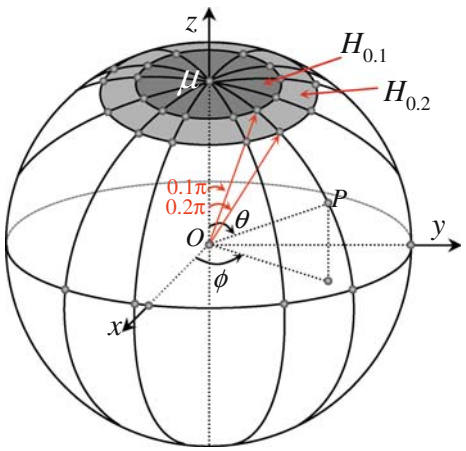

Fig. 4 Definition of $H_{0.1}$ and $H_{0.2}$ of the 3-D spherical data

$$H_{0.1} = \int_0^{2\pi}\int_0^{0.1\pi} f(\theta,\varphi)\sin\theta \, \mathrm{d}\theta \, \mathrm{d}\varphi,$$

$$H_{0.2} = \int_0^{2\pi}\int_0^{0.2\pi} f(\theta,\varphi)\sin\theta \, \mathrm{d}\theta \, \mathrm{d}\varphi. \quad (12)$$

Particular models for $f(\theta, \phi)$ are given in Appendix 2 for reference.

Examples

Size measurement

To demonstrate this methodology, homogeneity quantifications are made on two samples A and B, with different size distributions. The sample A contains particles with variable size. A representative TEM image is shown in Fig. 5a, and the measured histogram is shown in Fig. 5b, as compared with the calculated PDF's using normal, lognormal, gamma, and Weibull models, respectively. The measurement statistics are listed in Table 1. According to the measured ratio $\bar{x}/s = 2.008$, $H_{0.1}$ and $H_{0.2}$ are calculated by replacing $\bar{x}/s$ to μ/σ in the formulas in Appendix 1, as listed in Table 2 for different models. As the lognormal model gives the best fit, with the correlation coefficient [37] $r = 0.963$, which is the highest among others, the homogeneity of the sample A is quantified as $H_{0.1} = 16.5\%$ and $H_{0.2} = 32.9\%$ by the lognormal model.

Table 1 Measurement statistics of samples A and B in Fig. 5

Sample	$\bar{x}$ (μm)	s (μm)	$\bar{x}/s$	N
A	1.201	0.598	2.008	251
B	1.658	0.249	6.659	501

On the other hand, the sample B contains particles with a more homogeneous size. A representative TEM image is shown in Fig. 5c, and the measured histogram is shown in Fig. 5d, with the measurement statistics listed in Table 1. The measured ratio $\bar{x}/s = 6.659$, which is much higher that of the sample A. Calculated $H_{0.1}$ and $H_{0.2}$ are listed in Table 2, along with the correlation coefficient r of each model. Again the lognormal gives the best fit with $r = 0.965$, although the r values of the gamma and normal distributions are close to it. Therefore, the homogeneity of the sample B is quantified as $H_{0.1} = 49.8\%$ and $H_{0.2} = 82.5\%$ by the lognormal model, which are significantly higher than that of the sample A.

Here, we only calculate the H values from these four statistical models. Alternatively, one may calculate the experimental $H_{0.1}$ and $H_{0.2}$ values, i.e., the integrations of the measured histograms in the range $\bar{x} \pm 0.1\bar{x}$ and $\bar{x} \pm 0.2\bar{x}$, respectively. Therefore, if none of the existing models fits a distribution well, it is still possible to obtain the H values by integrating the histogram curves.

Note that here we only focus on the homogeneity degrees in the particle size, rather than their spacing. If one measures the spacing between these particles, the spacing homogeneity parameters $H_{0.1}$ and $H_{0.2}$ become the

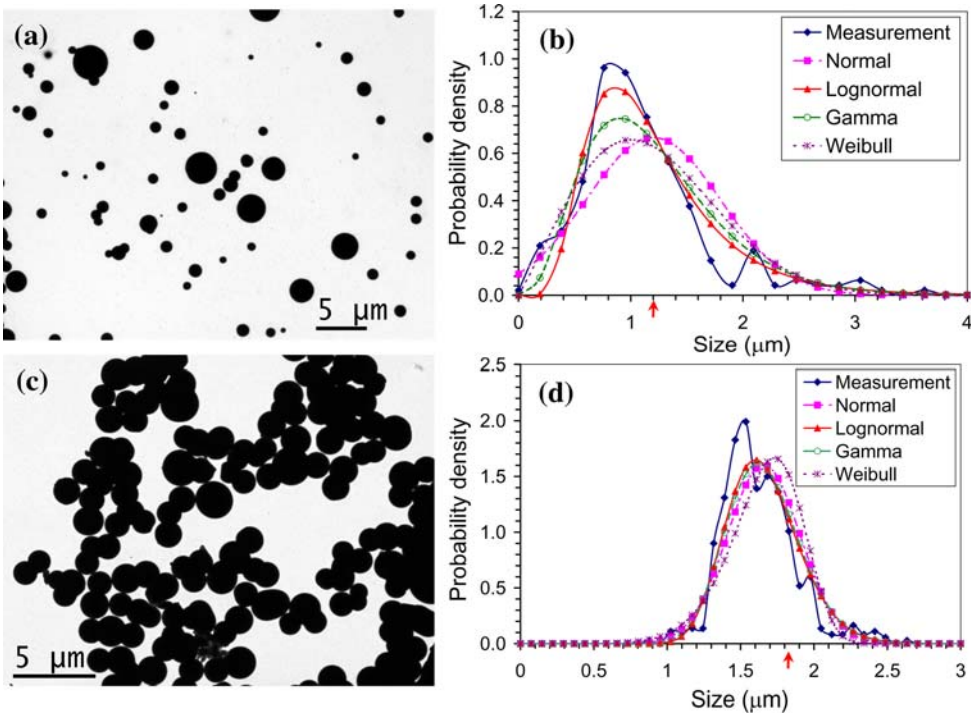

Fig. 5 **a** Representative TEM image of the sample A with variable size; **b** probability density distributions of the sample A; **c** representative TEM image of the sample B with homogeneous size; **d** probability density distribution of the sample B. Arrow indicates the mean size

Table 2 Homogeneity quantification of samples A and B in Fig. 5

Sample	Normal distribution			Lognormal distribution			Gamma distribution			Weibull distribution		
	$H_{0.1}$ (%)	$H_{0.2}$ (%)	r	$H_{0.1}$ (%)	$H_{0.2}$ (%)	r	$H_{0.1}$ (%)	$H_{0.2}$ (%)	r	$H_{0.1}$ (%)	$H_{0.2}$ (%)	r
A	15.9	31.2	0.842	16.5	32.9	0.963	15.6	30.8	0.941	15.0	29.6	0.901
B	49.5	81.7	0.938	49.8	82.5	0.965	49.5	82.0	0.957	49.5	82.6	0.885

dispersion parameters $D_{0.1}$ and $D_{0.2}$, respectively, as studied previously [23].

Axial data

Rigdahl et al. [13] studied the paper fiber distribution of 14 samples. Two of them, named as sample 80:3 and 80:1, respectively, with distinct different orientation distributions, are used as examples here for the axial data quantification. Their angular data were fitted using von Mises distribution,

$$f(\theta) = \frac{1}{\pi I_0(\kappa)} e^{\kappa \cos 2(\theta-\mu)}, \tag{13}$$

where I_0 is given in Eq. 38. Note that this equation for axial data is slightly different from Eq. 37 for directional data. The parameter κ, which controls the PDF shape, is found to be $\kappa = 0.14$ and 0.88 for the samples 80:3 and 80:1, respectively, and their PDFs are plotted in Fig. 6a and b, respectively. According to κ, their homogeneity degrees are calculated, as listed in Table 3. It is evident that the sample 80:1 has higher homogeneity degrees over the sample 80:3.

Based on the same experimental data, Schulgasser [14] fitted with the wrapped Cauchy model instead, which is expressed as:

$$f(\theta) = \frac{1}{\pi} \frac{1-\rho^2}{1+\rho^2-2\rho\cos 2(\theta-\mu)}. \tag{14}$$

The parameter ρ is found to be $\rho = 0.070$ and 0.374 for the sample 80:3 and 80:1, respectively. The PDFs of the wrapped Cauchy distribution are also plotted in Fig. 6.

Here, we add two more distribution models, wrapped normal and cardioid distributions. Wrapped normal distribution is expressed as:

$$f(\theta) = \frac{1}{\pi} + \frac{2}{\pi} \sum_{p=1}^{\infty} \rho^{p^2} \cos[2p(\theta-\mu)]. \tag{15}$$

Since its $\rho < 0.5$, cardioid distribution can also be used to model the data distribution as follows:

$$f(\theta) = \frac{1}{\pi}[1 + 2\rho\cos 2(\theta-\mu)]. \tag{16}$$

The homogeneity degrees are calculated according to ρ, as listed in Table 3. It is found that the wrapped Cauchy

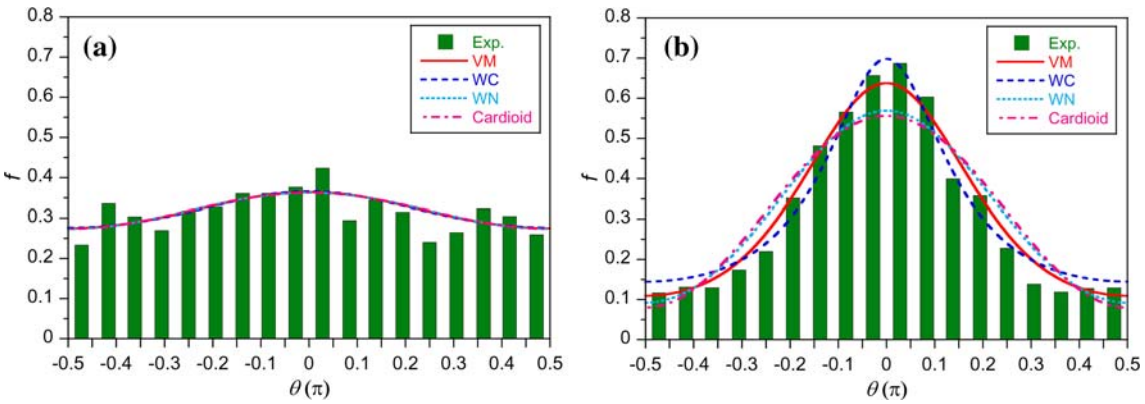

Fig. 6 Quantification of the orientation distributions of the samples 80:3 (**a**) and 80:1 (**b**)

Table 3 Homogeneity quantification of the axial data in Fig. 6

Sample	H_R (%)	von Mises distribution				Wrapped Cauchy distribution			Wrapped normal distribution			Cardioid distribution		
		κ	$H_{0.1}$ (%)	$H_{0.2}$ (%)	r	$H_{0.1}$ (%)	$H_{0.2}$ (%)	r	$H_{0.1}$ (%)	$H_{0.2}$ (%)	r	$H_{0.1}$ (%)	$H_{0.2}$ (%)	r
80:3 ($\rho = 0.070$)	7.0	0.14	11.7	23.3	0.983	11.6	22.7	0.984	11.4	22.6	0.983	11.4	22.6	0.983
80:1 ($\rho = 0.374$)	37.4	0.88	20.3	39.1	0.987	21.4	40.1	0.985	17.8	34.5	0.953	17.4	34.0	0.940

distribution gives best fit for the sample 80:3 with slightly higher correlation coefficient r, while the von Mises distribution gives best fit for the 80:1 sample. Using either H parameters, the sample 80:1 possesses higher homogeneity degrees over the sample 80:3.

Similar to the previous size measurement example, the $H_{0.1}$ and $H_{0.2}$ values can also be calculated by integrations in the measured histograms, regardless of the distribution model.

Directional data

The example of directional data is to quantify the line straightness, if the line is long enough to provide sufficient directional data. As shown in Fig. 7, a carbon nanofiber in Fig. 7a is straighter, while the one in Fig. 7b is more curved. As mentioned about Fig. 2e previously, the lines are divided into small sections and then the tangent direction angles at each point are measured using the program *ImageJ* [38]. The measured results are listed in Table 4, where H_R is simply quantified by $\overline{R}$. It is evident that the angles of the straight line in Fig. 7a are more concentrated, with $H_R = 97.3\%$, while angles of the curved line are less concentrated, with $H_R = 82.2\%$. As the angular data are nonsymmetrical, no effort is made to fit them using statistical models. This method by simply computing the H_R value can be used to evaluate single or bundle of linear features, such as nanotubes or nanowires [39, 40].

It is necessary to mention that, as the line straightness H has the opposite meaning of the curvature K, so the curvature can be obtained from H,

$$K = 1 - H. \tag{17}$$

However, the mathematical curvature is defined as:

$$K = \left|\frac{\Delta\theta}{\Delta L}\right|, \tag{18}$$

where $\Delta\theta$ and ΔL are the changes of angle and arc length, respectively, between two points. Its unit is the reciprocal of the measured length, thus the curvature K measured at different scale is not comparable. Besides, the measurement $\Delta\theta$ of two adjacent points would produce large error in practice. However, the straightness H and curvature $(1 - H)$ defined in this work are dimensionless, so they are comparable even at different scale.

Table 4 Quantification of the directional data in Fig. 7

Sample	Measurement			Straightness, H_R (%)	Curvature, $1 - H_R$ (%)
	$\overline{C}$	$\overline{S}$	N		
Straight fiber in Fig. 7a	0.8636	0.4478	95	97.3	2.7
Curved fiber in Fig. 7b	0.8063	0.1576	112	82.2	19.8

Summary of the work

Based on the homogeneity theory that the homogeneity degree is defined as the distribution probability, this work developed statistical approaches to compute the microstructural homogeneity degrees. Two types of important homogeneities are considered, for the size and orientations, respectively.

For the size distribution, it was proposed to quantify the homogeneity using two parameters, $H_{0.1}$ and $H_{0.2}$, which are defined as the probabilities falling into the ranges of $\mu \pm 0.1\mu$ and $\mu \pm 0.2\mu$, respectively. These quantities are formularized using different statistical models, as listed in Appendix 1. In the case of normal, lognormal, gamma (including its special cases of Erlang and chi-square), and Weibull (including its special case of Rayleigh) distributions, the homogeneity quantities $H_{0.1}$ and $H_{0.2}$ are found to be monotonic increasing functions of the ratio μ/σ. Therefore, depending on data distribution type, the homogeneity quantities $H_{0.1}$ and $H_{0.2}$ can be calculated from these equations by using $\overline{x}/s$ to replace μ/σ. Note that not all distributions possess the monotonic relationship between H and μ/σ, such as the beta distribution when $\alpha \neq \beta$. In this case, it is impossible to give the H values from the ratio μ/σ, i.e., a comparison of the homogeneity

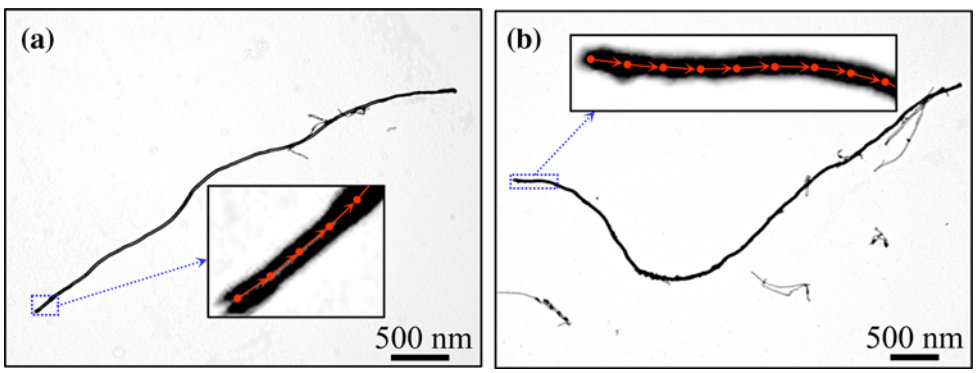

Fig. 7 Quantification of a straighter fiber in (**a**) and a curved fiber in (**b**)

solely by the ratio μ/σ or HPq is invalid. However, as a general way, the H values can be calculated by integrating $f(x)$ numerically as defined in Eq. 6.

For the orientation distribution, three parameters of H_R, $H_{0.1}$ and $H_{0.2}$ were defined. Either of them can quantify the homogeneity degree consistently. The first one H_R is a simple measure of the homogeneity of the angular data; while $H_{0.1}$ and $H_{0.2}$ are defined as the probabilities within certain angular data range as follows. (1) In case of 2-D circular data, if $0 \le \theta < 2\pi$ (directional data), $H_{0.1}$ and $H_{0.2}$ are defined as the probabilities within $\mu \pm 0.1\pi$ and $\mu \pm 0.2\pi$, respectively; while if $0 \le \theta < \pi$ (axial data), $H_{0.1}$ and $H_{0.2}$ are defined as the probabilities within $\mu \pm 0.05\pi$ and $\mu \pm 0.1\pi$, respectively. Therefore, one may denote the angle range of $H_{0.1}$ and $H_{0.2}$ as $\mu \pm 0.05\Delta\theta$ and $\mu \pm 0.1\Delta\theta$, respectively, where $\Delta\theta = \pi$ or $\Delta\theta = 2\pi$ for axial or directional data, respectively. These quantities are formularized in Appendix 2. (2) In case of 3-D spherical data, $H_{0.1}$ and $H_{0.2}$, are defined as probabilities for the colatitude θ range within 0.1π and 0.2π, respectively, from the mean direction μ. These quantities are also formularized in Appendix 2.

It is expected that the methodologies for the homogeneity quantification proposed in this article may be applicable beyond the scope of material microstructure. For example, the size homogeneity of objects seen in our daily life can be quantified in the same way as seen in the microscopic images. In fact, the linear feature quantification, as presented in Fig. 7, is similar to the case of the sedimentary structure along Vermilion River [36, 41] for earth science application. Generally, the H parameters defined in this work can quantitatively compare the homogeneity of any distribution, regardless of the object type.

Acknowledgement The author thanks three reviewers for their in-depth critical comments and constructive suggestions to improve this article.

Appendix 1: Size distribution

Normal and lognormal distribution

The normal and lognormal distributions were studied previously [23]. For a normal distribution,

$$H_{0.1} = 6.8843 \times 10^{-5} + 7.964 \times 10^{-2}(\mu/\sigma) + 1.043 \times 10^{-4}(\mu/\sigma)^2 - 1.6286 \times 10^{-4}(\mu/\sigma)^3 + 3.8639 \times 10^{-6}(\mu/\sigma)^4 \quad (r = 1), \tag{19a}$$

$$H_{0.2} = -4.0117 \times 10^{-4} + 0.16056(\mu/\sigma) - 2.8118 \times 10^{-4}(\mu/\sigma)^2 - 1.1826 \times 10^{-3}(\mu/\sigma)^3 + 5.6084 \times 10^{-5}(\mu/\sigma)^4 \quad (r = 1). \tag{19b}$$

For a lognormal distribution,

$$H_{0.1} = 1.1539 \times 10^{-2} + 7.5933 \times 10^{-2}(\mu/\sigma) + 6.6838 \times 10^{-4}(\mu/\sigma)^2 - 1.9169 \times 10^{-4}(\mu/\sigma)^3 + 3.9201 \times 10^{-6}(\mu/\sigma)^4 \quad (r = 0.99998), \tag{20a}$$

$$H_{0.2} = 2.266 \times 10^{-2} + 0.15629(\mu/\sigma) + 4.442 \times 10^{-4}(\mu/\sigma)^2 - 1.2738 \times 10^{-3}(\mu/\sigma)^3 + 5.9978 \times 10^{-5}(\mu/\sigma)^4 \quad (r = 0.99996). \tag{20b}$$

Gamma distribution

The density distribution of a gamma distribution is defined by

$$f(x) = \begin{cases} \frac{\beta^{-\alpha}}{\Gamma(\alpha)} x^{\alpha-1} e^{-x/\beta}, & \text{if } x > 0, \\ 0, & \text{if } x \le 0. \end{cases} \tag{21}$$

Its mean and variance are

$$\mu = \alpha\beta,\ \sigma^2 = \alpha\beta^2. \tag{22}$$

Here, the gamma function $\Gamma(\alpha)$ in Eq. 21 is expressed as $\Gamma(\alpha) = \int_0^\infty t^{\alpha-1} e^{-t}\, dt$. The probability distribution function for the gamma distribution is $F(x) = 0$ for $x \le 0$ and $F(x) = \gamma(\frac{x}{\beta}; \alpha)$ for $x > 0$. Here, γ is the incomplete gamma function, $\gamma(x;\alpha) = \frac{1}{\Gamma(\alpha)} \int_0^x t^{\alpha-1} e^{-t}\, dt$, whose value can be found in statistical references or online programs.

From Eq. 22, $\mu/\sigma = \sqrt{\alpha}$, thus $\alpha = (\mu/\sigma)^2$. Hence, the homogeneity

$$H_{0.1} = F(1.1\mu) - F(0.9\mu) = \gamma(1.1\alpha;\alpha) - \gamma(0.9\alpha;\alpha) = \gamma[1.1(\mu/\sigma)^2; (\mu/\sigma)^2] - \gamma[0.9(\mu/\sigma)^2; (\mu/\sigma)^2], \tag{23a}$$

$$H_{0.2} = F(1.2\mu) - F(0.8\mu) = \gamma(1.2\alpha;\alpha) - \gamma(0.8\alpha;\alpha) = \gamma[1.2(\mu/\sigma)^2; (\mu/\sigma)^2] - \gamma[0.8(\mu/\sigma)^2; (\mu/\sigma)^2]. \tag{23b}$$

From these two equations, $H_{0.1}$ and $H_{0.2}$ are functions of a single variable μ/σ. For convenience, they are regressed as

$$H_{0.1} = -8.1378 \times 10^{-3} + 8.2576 \times 10^{-2}(\mu/\sigma) - 1.335 \times 10^{-4}(\mu/\sigma)^2 - 1.7388 \times 10^{-4}(\mu/\sigma)^3 + 5.3408 \times 10^{-6}(\mu/\sigma)^4 \quad (r = 0.99999), \tag{24a}$$

$$H_{0.2} = -1.7039 \times 10^{-2} + 0.16844(\mu/\sigma) - 9.1716 \times 10^{-4}(\mu/\sigma)^2 - 1.2346 \times 10^{-3}(\mu/\sigma)^3 + 6.1571 \times 10^{-5}(\mu/\sigma)^4 \quad (r = 0.99997). \tag{24b}$$

Note that the gamma distribution yields a special case of Erlang distribution when $\alpha = k$ is an integer, or the chi-square distribution when $\alpha = v/2$ and $\beta = 2$ [24]. As $H_{0.1}$ and $H_{0.2}$ are only related to the ratio μ/σ but not related to specific α or β, the homogeneity equations, as expressed in Eqs. 23a, 23b and 24a, 24b, remain valid for both Erlang and chi-square distributions.

Weibull distribution

The density distribution of a Weibull distribution is defined by:

$$f(x)=\begin{cases}\alpha\beta^{-\alpha}x^{\alpha-1}\mathrm{e}^{-(x/\beta)^{\alpha}}, & \text{if } x>0,\\ 0, & \text{if } x\le 0.\end{cases} \quad (25)$$

Its mean and variance are

$$\mu=\beta\Gamma\left(\frac{\alpha+1}{\alpha}\right),\sigma^2=\beta^2\left[\Gamma\left(\frac{\alpha+2}{\alpha}\right)-\Gamma^2\left(\frac{\alpha+1}{\alpha}\right)\right]. \quad (26)$$

Thus, we have

$$(\mu/\sigma)=\frac{\Gamma\left(\frac{\alpha+1}{\alpha}\right)}{\sqrt{\Gamma\left(\frac{\alpha+2}{\alpha}\right)-\Gamma^2\left(\frac{\alpha+1}{\alpha}\right)}},\ \text{or}\ \frac{1+(\mu/\sigma)^2}{(\mu/\sigma)^2}=\frac{\Gamma\left(\frac{\alpha+2}{\alpha}\right)}{\Gamma^2\left(\frac{\alpha+1}{\alpha}\right)}. \quad (27)$$

From Eq. 27, the relationship between α and (μ/σ) can be established, and their relationship is expressed as:

$$\begin{aligned}\alpha=&\,8.8947\times10^{-2}+0.8434(\mu/\sigma)+0.10306(\mu/\sigma)^2\\&-1.0683\times10^{-2}(\mu/\sigma)^3\\&+4.0045\times10^{-4}(\mu/\sigma)^4\quad(r=1).\end{aligned} \quad (28)$$

The probability distribution function for the Weibull distribution is $F(x)=0$ for $x\le 0$ and $F(x)=1-\mathrm{e}^{-(x/\beta)^{\alpha}}$ for $x>0$. Therefore, the homogeneity degree of the Weibull distribution is:

$$\begin{aligned}H_{0.1}&=F(1.1\mu)-F(0.9\mu)=\mathrm{e}^{-(0.9\mu/\beta)^{\alpha}}-\mathrm{e}^{-(1.1\mu/\beta)^{\alpha}}\\&=\mathrm{e}^{-\left[0.9\Gamma\left(\frac{\alpha+1}{\alpha}\right)\right]^{\alpha}}-\mathrm{e}^{-\left[1.1\Gamma\left(\frac{\alpha+1}{\alpha}\right)\right]^{\alpha}},\end{aligned} \quad (29a)$$

$$\begin{aligned}H_{0.2}&=F(1.2\mu)-F(0.8\mu)=\mathrm{e}^{-(0.8\mu/\beta)^{\alpha}}-\mathrm{e}^{-(1.2\mu/\beta)^{\alpha}}\\&=\mathrm{e}^{-\left[0.8\Gamma\left(\frac{\alpha+1}{\alpha}\right)\right]^{\alpha}}-\mathrm{e}^{-\left[1.2\Gamma\left(\frac{\alpha+1}{\alpha}\right)\right]^{\alpha}}.\end{aligned} \quad (29b)$$

Here, $\mu/\beta=\Gamma\left(\frac{\alpha+1}{\alpha}\right)$ according to Eq. 26. For a given μ/σ, the value α can be evaluated from Eq. 28, and thus $H_{0.1}$ and $H_{0.2}$ can be calculated. For convenience, these equations are regressed as:

$$\begin{aligned}H_{0.1}=&\,2.0549\times10^{-3}+6.9954\times10^{-2}(\mu/\sigma)\\&+2.6087\times10^{-3}(\mu/\sigma)^2-3.663\times10^{-4}(\mu/\sigma)^3\\&+1.0206\times10^{-5}(\mu/\sigma)^4\quad(r=1),\end{aligned} \quad (30a)$$

$$\begin{aligned}H_{0.2}=&\,5.975\times10^{-3}+0.13709(\mu/\sigma)\\&+7.1542\times10^{-3}(\mu/\sigma)^2-1.8982\times10^{-3}(\mu/\sigma)^3\\&+7.6268\times10^{-5}(\mu/\sigma)^4\quad(r=1).\end{aligned} \quad (30b)$$

Note that the Weibull distribution yields a special case, Rayleigh distribution, by taking $\alpha=2$ and $\beta=\sqrt{2}\eta$ [24]. As $H_{0.1}$ and $H_{0.2}$ are not related to specific α or β values in these H equations, they can also be used for the homogeneity quantification of the Rayleigh distribution.

Beta distribution

The beta distribution is defined as:

$$f(x)=\frac{1}{B(\alpha,\beta)}x^{\alpha-1}(1-x)^{\beta-1},\quad 0<x<1, \quad (31)$$

where α and β are two independent fitting parameters, and $B(\alpha,\beta)=\Gamma(\alpha)\Gamma(\beta)/\Gamma(\alpha+\beta)$. Its mean $\mu=\alpha/(\alpha+\beta)$ and variance $\sigma^2=\alpha\beta/[(\alpha+\beta)^2(\alpha+\beta+1)]$, and thus $(\mu/\sigma)^2=\alpha(\alpha+\beta+1)/\beta$. For a given pair of α and β, particular H values can be computed numerically by integrating $f(x)$ in Eq. 31 over the range of $\mu\pm0.1\mu$ or $\mu\pm0.2\mu$. Figure 8 shows some of the computation results of the beta distribution for $0<\alpha,\ \beta\le10$, as plotted as H versus $(\mu/\sigma)=\sqrt{\alpha(\alpha+\beta+1)/\beta}$. The normal distribution is included for comparison. Different to the previous distributions, the homogeneity parameters $H_{0.1}$ and $H_{0.2}$ here are functions of the ratio μ/σ as well as α (or β), i.e., for a given μ/σ, $H_{0.1}$, and $H_{0.2}$ are no longer monotonic but may possess different values depending on α or β. Only when $\alpha=\beta$, $H_{0.1}$ and $H_{0.2}$ are monotonic functions of μ/σ, which as expressed as:

$$\begin{aligned}H_{0.1}=&-0.19399+0.2557(\mu/\sigma)-0.072226(\mu/\sigma)^2\\&+1.5503\times10^{-2}(\mu/\sigma)^3-1.8411\times10^{-3}(\mu/\sigma)^4\\&+1.1168\times10^{-4}(\mu/\sigma)^5-2.7194\times10^{-6}(\mu/\sigma)^6\\&(r=0.99999),\end{aligned} \quad (32a)$$

$$\begin{aligned}H_{0.2}=&-0.3923+0.51722(\mu/\sigma)-0.14489(\mu/\sigma)^2\\&+3.0054\times10^{-2}(\mu/\sigma)^3-3.6426\times10^{-3}(\mu/\sigma)^4\\&+2.2641\times10^{-4}(\mu/\sigma)^5-5.604\times10^{-6}(\mu/\sigma)^6\\&(r=0.99998).\end{aligned} \quad (32b)$$

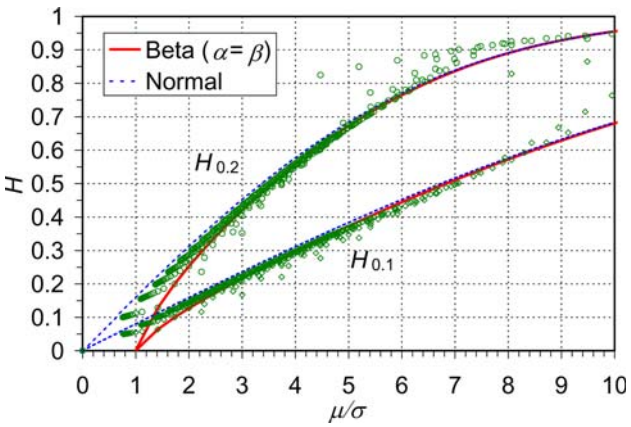

Fig. 8 Homogeneity quantities $H_{0.1}$ and $H_{0.2}$ of the beta distribution, as compared with the normal distribution. Each *dot* corresponds to a pair of (α, β) values (not shown), while a special case with $\alpha=\beta$ is highlighted

As shown in Fig. 8, the H values with $\alpha = \beta$ are highlighted, which are getting close to the normal distribution at higher ratio μ/σ.

Moreover, the homogeneity H functions of the uniform, exponential, Laplace, Pareto, or any other distributions [24] can be formularized from their specific integration forms, while these models are not commonly used for the size distribution modeling.

Appendix 2: Orientation distribution

Circular data

Wrapped normal distribution

The density distribution of the wrapped normal distribution is described as

$$f(\theta) = \frac{1}{2\pi} + \frac{1}{\pi}\sum_{p=1}^{\infty} \rho^{p^2} \cos[p(\theta - \mu)],$$
$$0 \le \theta < 2\pi,\ 0 \le \rho \le 1. \tag{33}$$

Its mean is μ, and mean resultant length is ρ. By numerical computation, the relationship of H_R, $H_{0.1}$, and $H_{0.2}$ with ρ are obtained, as shown in Fig. 9, which are expressed as follows:

$$H_R = \rho, \tag{34a}$$

$$H_{0.1} = 0.10011 + 0.047109\rho + 4.4886\rho^2 - 45.267\rho^3 + 216.03\rho^4 - 549.16\rho^5 + 766.28\rho^6 - 553.37\rho^7 + 161.92\rho^8 \quad (r = 0.99995), \tag{34b}$$

$$H_{0.2} = 0.19979 + 0.6295\rho - 7.1152\rho^2 + 67.738\rho^3 - 305.85\rho^4 + 738.89\rho^5 - 977.14\rho^6 + 667.18\rho^7 - 183.52\rho^8 \quad (r = 0.99997). \tag{34c}$$

Wrapped Cauchy distribution

The density distribution of the wrapped Cauchy distribution, with mean direction μ and mean resultant length ρ, is described as:

$$f(\theta) = \frac{1}{2\pi}\frac{1-\rho^2}{1+\rho^2-2\rho\cos(\theta-\mu)},$$
$$0 \le \theta < 2\pi,\ 0 \le \rho \le 1. \tag{35}$$

The relationships of H_R, $H_{0.1}$ and $H_{0.2}$ with ρ are shown in Fig. 10, which are expressed as follows:

$$H_R = \rho, \tag{36a}$$

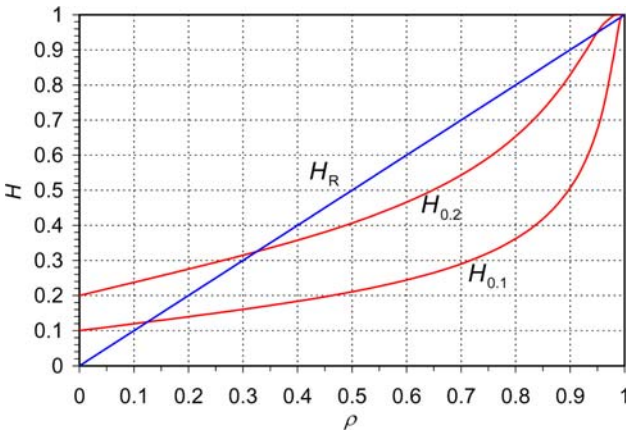

Fig. 9 Homogeneity H of wrapped normal distribution

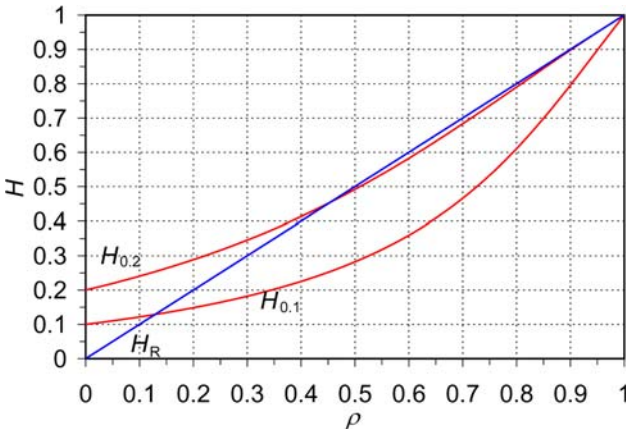

Fig. 10 Homogeneity H of wrapped Cauchy distribution

$$H_{0.1} = 0.1 + 0.25447\rho - 0.57728\rho^2 + 4.1115\rho^3 - 9.2654\rho^4 + 10.617\rho^5 - 4.2392\rho^6 \quad (r = 0.99999), \tag{36b}$$

$$H_{0.2} = 0.2 + 0.36274\rho + 0.45329\rho^2 - 0.56551\rho^3 + 1.8836\rho^4 - 0.8692\rho^5 + 0.53479\rho^6 \quad (r = 1). \tag{36c}$$

von Mises distribution

The widely used von Mises distribution, with mean direction μ, is described by a density function of

$$f(\theta) = \frac{1}{2\pi I_0(\kappa)} e^{\kappa\cos(\theta-\mu)}, \quad 0 \le \theta < 2\pi,\ 0 \le \kappa < \infty, \tag{37}$$

where I_0 denotes the modified Bessel function of the first kind, with order 0 ($p = 0$). In general with the order p, it is defined by

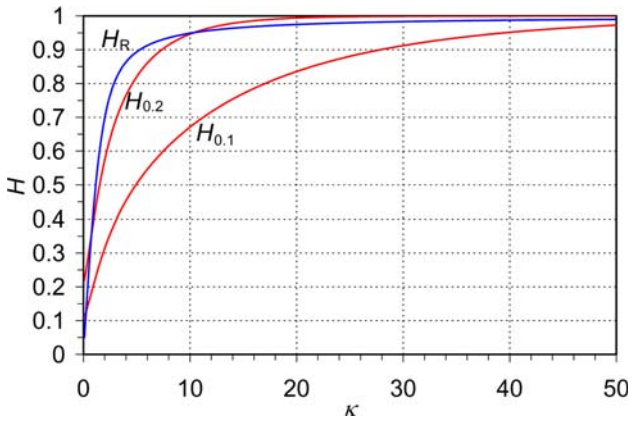

Fig. 11 Homogeneity H of von Mises distribution

$$I_p(\kappa) = \frac{1}{2\pi}\int_0^{2\pi} \cos p\theta \, e^{\kappa\cos\theta} d\theta, \text{ or}$$

$$I_p(\kappa) = \sum_{r=0}^{\infty} \frac{1}{\Gamma(p+r+1)\Gamma(r+1)}\left(\frac{\kappa}{2}\right)^{2r+p}. \quad (38)$$

Its mean resultant length is $\rho = I_1(\kappa)/I_0(\kappa)$. According to these relationships, H_R, $H_{0.1}$, and $H_{0.2}$ are numerically computed, as shown in Fig. 11. In the range of $\kappa \le 20$ that covers most practical values, they are expressed as:

$$\begin{aligned} H_R = \rho = {} & 0.62021\kappa - 0.18640\kappa^2 + 3.1477\times10^{-2}\kappa^3 \\ & - 3.177\times10^{-3}\kappa^4 + 1.9433\times10^{-4}\kappa^5 \\ & - 6.9914\times10^{-6}\kappa^6 + 1.3417\times10^{-7}\kappa^7 \\ & - 1.0355\times10^{-9}\kappa^8 \quad (r = 0.99955), \end{aligned} \quad (39a)$$

$$\begin{aligned} H_{0.1} = {} & 0.1 + 0.12268\kappa - 3.56\times10^{-3}\kappa^2 \\ & - 3.1725\times10^{-3}\kappa^3 + 7.3794\times10^{-4}\kappa^4 \\ & - 7.7475\times10^{-5}\kappa^5 + 4.3665\times10^{-6}\kappa^6 \\ & - 1.2782\times10^{-7}\kappa^7 + 1.527\times10^{-9}\kappa^8 \\ & (r = 0.99996), \end{aligned} \quad (39b)$$

$$\begin{aligned} H_{0.2} = {} & 0.2 + 0.23837\kappa - 2.1741\times10^{-2}\kappa^2 \\ & - 3.3761\times10^{-3}\kappa^3 + 1.1134\times10^{-3}\kappa^4 \\ & - 1.2683\times10^{-4}\kappa^5 + 7.4053\times10^{-6}\kappa^6 \\ & - 2.2105\times10^{-7}\kappa^7 + 2.674\times10^{-9}\kappa^8 \\ & (r = 0.99978). \end{aligned} \quad (39c)$$

Cardioid distribution

The cardioid distribution, with a mean direction at μ, has the density function as follows:

$$f(\theta) = \frac{1}{2\pi}[1 + 2\rho\cos(\theta - \mu)], \quad 0 \le \theta < 2\pi, \ |\rho| \le \frac{1}{2}. \quad (40)$$

Its mean resultant length is ρ, thus

$$H_R = \rho. \quad (41a)$$

According to Eq. 40, the density function at $\rho = 0.5, 0, -0.5$ are shown in Fig. 12a. When $\rho = 0.5$, the maximum f is at $\theta = 0$, so $\mu = 0$. Therefore, $H_{0.1}$ and $H_{0.2}$ include areas on the right side of $\theta = 0$ and left side of $\theta = 2\pi$, as shown in the shadowed areas in Fig. 12a. While when $\rho = -0.5$, $H_{0.1}$ and $H_{0.2}$ are obtained from the areas with $\mu = \pi$. Along with H_R, the calculated results of $H_{0.1}$ and $H_{0.2}$ are shown in Fig. 12b, which are computed as:

$$H_{0.1} = 0.1 + 0.19673|\rho| \quad (r = 1), \quad (41b)$$

$$H_{0.2} = 0.2 + 0.374196|\rho| \quad (r = 1). \quad (41c)$$

Triangle distribution

The triangle distribution, with mean direction at μ, has the density function as follows [33]:

$$f(\theta) = \frac{1}{8\pi}\left(4 - \pi^2\rho + 2\pi\rho|\pi - \theta|\right),$$
$$0 \le \theta < 2\pi, \ 0 \le \rho \le \frac{4}{\pi^2}. \quad (42)$$

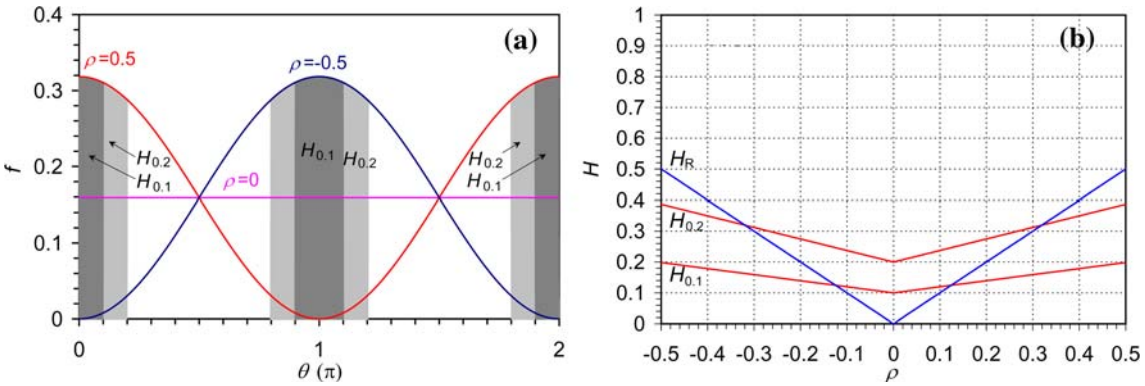

Fig. 12 PDF (**a**) and homogeneity H (**b**) of cardioid distribution

From this function, it is computed that

$$H_R = \rho, \tag{43a}$$

$$H_{0.1} = 0.1 + 0.22209\rho \quad (r = 1), \tag{43b}$$

$$H_{0.2} = 0.2 + 0.39522\rho \quad (r = 1). \tag{43c}$$

For other distribution models, H_R, $H_{0.1}$, and $H_{0.2}$ then can be computed in similar ways. Even when the ρ of a model is not available, for example, the nonsymmetrical models given by Fu and Lauke [8], the $H_{0.1}$ and $H_{0.2}$ can be calculated numerically.

Spherical data

Fisher distribution

The density function of Fisher distribution [35], with mean direction along the z axis, is expressed as:

$$f(\theta, \varphi) = (\kappa/4\pi\sinh\kappa)\exp(\kappa\cos\theta)\sin\theta, \tag{44}$$

where κ is the concentration parameter, which controls the curved shape, as plotted for some values in Fig. 13a. Its

$$H_R = \rho = \coth\kappa - 1/\kappa. \tag{45a}$$

Accordingly, the H values are calculated for different κ (Fig. 13b), and regressed as:

$$\begin{aligned} H_{0.1} = {} & 1.2994 \times 10^{-2} + 4.4163 \times 10^{-2}\kappa \\ & - 5.0189 \times 10^{-4}\kappa^2 - 2.6177 \times 10^{-5}\kappa^3 \\ & + 1.3518 \times 10^{-6}\kappa^4 - 2.9028 \times 10^{-8}\kappa^5 \\ & + 3.335 \times 10^{-10}\kappa^6 - 1.9918 \times 10^{-12}\kappa^7 \\ & + 4.8533 \times 10^{-15}\kappa^8 \quad (r = 0.99999), \end{aligned} \tag{45b}$$

$$\begin{aligned} H_{0.2} = {} & 0.060241 + 0.15876\kappa - 1.1775 \times 10^{-2}\kappa^2 \\ & + 4.8757 \times 10^{-4}\kappa^3 - 1.2163 \times 10^{-5}\kappa^4 \\ & + 1.8637 \times 10^{-7}\kappa^5 - 1.7134 \times 10^{-9}\kappa^6 \\ & + 8.6621 \times 10^{-12}\kappa^7 - 1.8495 \times 10^{-14}\kappa^8 \\ & (r = 0.99987). \end{aligned} \tag{45c}$$

Watson distribution

The density function of Watson distribution [35], with mean direction along the z-axis, is expressed as

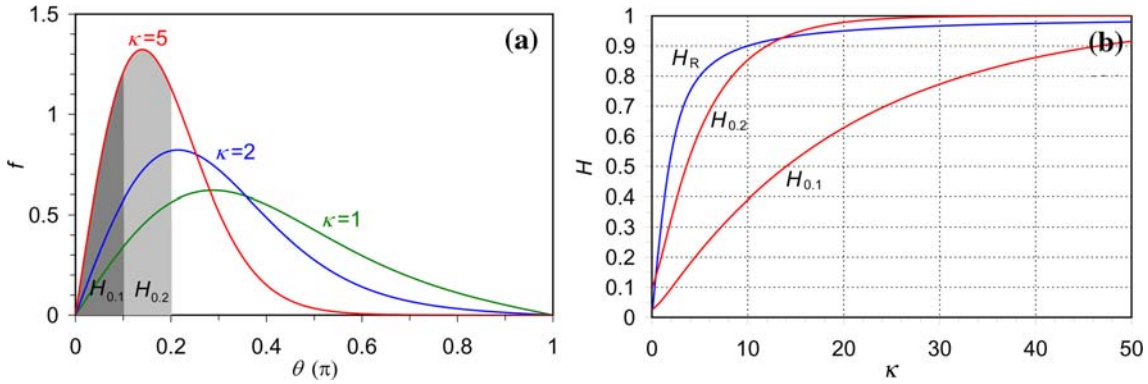

Fig. 13 PDF (**a**) and homogeneity H (**b**) of Fisher distribution

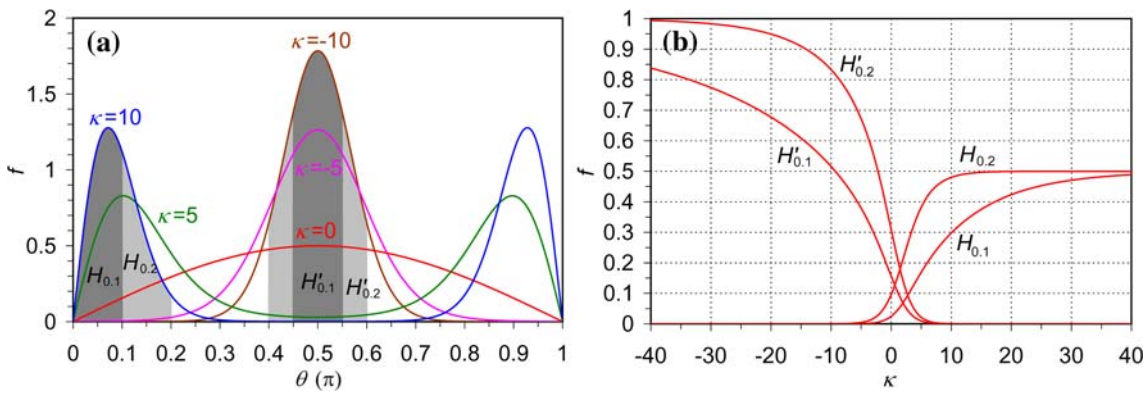

Fig. 14 PDF (**a**) and homogeneity H (**b**) of Watson distribution

$$f(\theta,\varphi) = C_{\mathrm{W}}\exp(\kappa\cos^2\theta)\sin\theta, \tag{46}$$

where $C_{\mathrm{W}} = 1/[4\pi\int_0^1 \exp(\kappa u^2)\mathrm{d}u]$. When $\kappa \geq 0$, the distribution f is plotted in Fig. 14a, with $H_{0.1}$ and $H_{0.2}$ areas indicated. As the another half at the supplementary angle $(\pi - \theta)$ in not included, the maximum H value is 0.5. Its ρ is not available. However, the H quantities are calculated numerically as shown in Fig. 14b for $0 \leq \kappa \leq 40$, which are expressed as:

$$\begin{aligned} H_{0.1} &= 2.469\times10^{-2} + 1.2754\times10^{-2}\kappa \\ &\quad + 7.0861\times10^{-3}\kappa^2 - 1.1119\times10^{-3}\kappa^3 \\ &\quad + 8.2392\times10^{-5}\kappa^4 - 3.5013\times10^{-6}\kappa^5 \\ &\quad + 8.6587\times10^{-8}\kappa^6 - 1.1573\times10^{-9}\kappa^7 \\ &\quad + 6.4609\times10^{-12}\kappa^8 \quad (r = 1), \end{aligned} \tag{47a}$$

$$\begin{aligned} H_{0.2} &= 9.5345\times10^{-2} + 4.3964\times10^{-2}\kappa \\ &\quad + 1.4318\times10^{-2}\kappa^2 - 3.9435\times10^{-3}\kappa^3 \\ &\quad + 4.3047\times10^{-4}\kappa^4 - 2.6193\times10^{-5}\kappa^5 \\ &\quad + 9.5653\times10^{-7}\kappa^6 - 2.0844\times10^{-8}\kappa^7 \\ &\quad + 2.5002\times10^{-10}\kappa^8 - 1.2709\times10^{-12}\kappa^9 \\ &\quad (r = 0.99997). \end{aligned} \tag{47b}$$

However when $\kappa < 0$, as plotted in Fig. 14a, the f maximum value is at 0.5π, i.e., at the equator, which is the girdle case. It is more reasonable to define the homogeneity, denoted as H', around 0.5π, as shown in Fig. 14a. Within $-40 \leq \kappa < 0$, the H' is expressed as:

$$\begin{aligned} H'_{0.1} &= 0.15391 - 5.833\times10^{-2}\kappa - 3.2517\times10^{-3}\kappa^2 \\ &\quad - 1.3384\times10^{-4}\kappa^3 - 3.4286\times10^{-6}\kappa^4 \\ &\quad - 4.7827\times10^{-8}\kappa^5 - 2.7634\times10^{-10}\kappa^6 \\ &\quad (r = 1), \end{aligned} \tag{48a}$$

$$\begin{aligned} H'_{0.2} &= 0.30501 - 0.10639\kappa - 8.3415\times10^{-3}\kappa^2 \\ &\quad - 3.9327\times10^{-4}\kappa^3 - 1.0983\times10^{-5}\kappa^4 \\ &\quad - 1.6572\times10^{-7}\kappa^5 - 1.0359\times10^{-9}\kappa^6 \\ &\quad (r = 0.99999). \end{aligned} \tag{48b}$$

References

1. Underwood EE (1970) Quantitative stereology. Addison-Wesley, Reading
2. Takayama Y, Tozawa T, Kato H, Akaneya Y, Chang IS (1996) J Japn Inst Met 60:44 (in Japanese)
3. Heijman MJGW, Benes NE, ten Elshof JE, Verweij H (2002) Mater Res Bull 37:141
4. Hendriks MGHM, Heijman MJGW, van Zyl WE, ten Elshof JE, Verweij H (2002) J Am Ceram Soc 85:2097
5. Sidor Y, Dzubinsky M, Kovac F (2003) Mater Charact 51:109
6. Sidor Y, Dzubinsky M, Kovac F (2005) J Mater Sci 40:6257. doi:10.1007/s10853-005-3145-7
7. Gadala-Maria F, Parsi F (1993) Polym Compos 14:126
8. Fu SY, Lauke B (1996) Compos Sci Technol 56:1179
9. Kim HS (2004) Fiber Polym 5:177
10. Reihanian M, Ebrahimi R, Moshksar MM, Terada D, Tsuji N (2008) Mater Charact 59:1312
11. Luo ZP (2006) Acta Mater 54:47
12. Suzuki S, Takeda K (2000) J Wood Sci 46:289
13. Rigdahl M, Andersson H, Westerlind B, Hollmark H (1983) Fibre Sci Technol 19:127
14. Schulgasser K (1985) J Mater Sci 20:859. doi:10.1007/BF00585727
15. Russ JC (1991) Mater Charact 27:185
16. Carpenter DT, Rickman JM, Barmak K (1998) J Appl Phys 84:5843
17. Roebuck B (2000) Mater Sci Technol 16:1167
18. Takahashi J, Suito H (2001) Acta Mater 49:711
19. Chen SP, Hanlon DN, Van der Zwaag S, Pei YT, Dehosson JTM (2002) J Mater Sci 37:989. doi:10.1023/A:1014356116058
20. Susan D (2005) Metall Mater Trans A 36:2481
21. Duarte MT, Liu HY, Kou SQ, Lindqvist PA, Miskovsky K (2005) J Mater Eng Perform 14:104
22. Zhilyaev AP, Swaminathan S, Gimazov AA, McNelley TR, Langdon TG (2008) J Mater Sci 43:7451. doi:10.1007/s10853-008-2714-y
23. Luo ZP, Koo JH (2007) J Microsc 225:118
24. Dougherty ER (1990) Probability and statistics for the engineering, computing, and physical sciences. Prentic-Hall, Inc., Englewood Cliffs, New Jersey
25. Schwarz H, Exner HE (1983) J Microsc 129:155
26. Yang N, Boselli J, Sinclair I (2001) J Microsc 201:189
27. Ganguly P, Poole WJ (2002) Mater Sci Eng A332:301
28. Luo ZP, Koo JH (2008) Mater Lett 62:3493
29. Luo ZP, Koo JH (2008) Polymer 49:1841
30. Morawiec A (2004) Orientations and rotations: computations in crystallographic textures. Springer, Berlin
31. Fisher NI (1993) Statistical analysis of circular data. Cambridge University Press, Cambridge
32. Mardia KV, Jupp PE (2000) Directional statistics. Wiley, West Sussex, England
33. Jammalamadaka SR, SenGupta A (2001) Topics in circular statistics. World Scientific Publishing Co., Pte. Ltd., Singapore
34. Watson GS (1983) Statistics on spheres. Wiley, New York
35. Fisher NI, Lewis T, Embleton BJJ (1987) Statistical analysis of spherical data. Cambridge University Press, Cambridge
36. Borradaile G (2003) Statistics of earth science data: their distribution in time, space, and orientation. Springer, Berlin
37. Nelson PR, Coffin M, Copeland KAF (2003) Introductory statistics for engineering experimentation. Elsevier, Amsterdam
38. Abramoff MD, Magelhaes PJ, Ram SJ (2004) Biophoton Int 11:36
39. Al-Khedher MA, Pezeshki C, McHale JL, Knorr FJ (2007) Nanotechnology 18:355703 (11pp)
40. Chen SH, Chen CC, Luo ZP, Chao CG (2009) Mater Lett 63:1165
41. Potter PE, Pettijohn FJ (1977) Paleocurrents and basin analysis. Springer, Berlin